A Comprehensive Analysis of Binary Mixtures as Working Fluid in High Temperature Heat Pumps

Hamed Abedini[a], Elias Vieren[b], Toon Demeester[b], Wim Beyne[b], Steven Lecompte[b, c], Sylvain Quoilin[a], Alessia Arteconi[a,d,e,*]

[a] *Mechanical Engineering Department, KU Leuven, Leuven 3000, Belgium*

[b] *Department of Electromechanical, Systems and Metal Engineering, Ghent University, Gent 9000, Belgium*

[c] *FlandersMake @ UGENT – Core lab EEDT – MP, Leuven 3000, Belgium*

[d] *Dipartimento di Ingegneria Industriale e Scienze Matematiche, Università Politecnica delle Marche, 60131, Ancona, Italy*

[e] *EnergyVille, 3600, Genk, Belgium*

** Corresponding author. Email address: alessia.arteconi@kuleuven.be, Tel.: +32 14 72 14 68*

Abstract

High-temperature heat pumps represent an emerging technology with a great potential in supplying clean heat to energy intensive industries. Suitable refrigerants for high-temperature heat pumps (up to 200°C) have not been identified yet. This work aims to analyze the performance of binary mixtures as working fluid in high-temperature heat pumps delivering heat up to 200°C with a special focus on zeotropic mixtures. Three relevant processes with different heat sources and sinks were selected to integrate the heat pump: latent/latent (e.g. distillation processes), latent/sensible (e.g. superheated steam drying), sensible/sensible (e.g. pressurized water production). To determine the best working fluid and cycle configuration for each process, an optimization framework was developed with the maximization of the coefficient of performance as objective function. For the first case with a latent heat sink and heat source, the best performing binary mixtures were near-azeotropic with slightly higher coefficient of performance compared to pure fluids. Moreover, binary mixtures provided several advantages such as the reduction of the compression ratio and compressor outlet temperature compared to pure fluids. A similar behavior was observed for the second case with a latent heat source and a sensible heat sink. For the third case with a sensible heat sink and heat source, binary mixtures resulted in a higher coefficient of performance (10%) compared to pure fluids. Most of the best performing mixtures were hydrocarbons with high risk of flammability. Water/ammonia was the only mildly-flammable mixture among the top mixtures.

Keywords: high-temperature heat pump, temperature glide, optimization, zeotropic mixture, thermodynamics

Nomenclature

Symbols:

h	*specific enthalpy*	*[kJ/kg]*
$\dot{m}$	*mass flow rate*	*[kg/s]*
p	*pressure*	*[bar]*
T	*temperature*	*[°C]*
x_{mole}	*mole fraction of the first component in liquid phase*	*[-]*
y_{mole}	*mole fraction of the first component in vapor phase*	*[-]*
z_{mole}	*mole fraction of the first component*	*[-]*
α	*relative volatility*	*[-]*
η	*efficiency*	*[-]*
ρ	*density*	*[kg/m³]*

Subscripts

c	*compressor*
cd	*condenser*
cr	*critical*
ev	*evaporator*
in	*inlet*
is	*isentropic*
out	*outlet*
sc	*subcooling*
sh	*superheat*
si	*sink*
so	*source*

Abbreviations:

COP	*coefficient of performance*
DWC	*dividing-wall column*
GWP	*global warming potential*
HTHP	*high-temperature heat pump*
IHX	*internal heat exchanger*
MTA	*minimum temperature approach*
ODP	*ozone depletion potential*
PHWP	*pressurized hot water production*
SSD	*superheated steam drying*
TXV	*thermal expansion valve*
VHC	*volumetric heating capacity*

1. Introduction

Industrial thermal processes are responsible for around 24% of the total heating and cooling needs in EU [1] and they still largely rely on fossil fuels. The rising concerns for greenhouse gas emissions, together with the global growth of energy demand are leading to a necessary shift towards sustainable alternatives in the industrial heating sector. In this regard, G.P. Thiel et al. [2] identified four pillars for the decarbonization of industrial processes: (1) zero-carbon heat, (2) electrification of heat, (3) zero-carbon fuels, and (4) better heat management. Among the abovementioned research areas, the deep electrification of industry is considered of utmost importance and it would allow the integration of higher shares of renewables for heating purposes [3]. In particular, the integration of high-temperature heat pumps is considered one of the most promising options for the decarbonization of low and medium temperature industrial heat thanks to the high efficiencies and to the possibility to recover and upgrade on-site waste heat sources [2]. F. Bühler et al. [4] analysed the electrification potential of the Danish industry, demonstrating that heat pumps could cover a significant share of the total process heat demand. The large-scale deployment of these devices would significantly reduce greenhouse gases emissions, lead to energy savings and increased overall efficiency for the involved industrial actors.

Heat pumps can be classified based on the temperature level of the heat delivered. When the useful heat produced by heat pumps exceeds 100°C, the literature typically refers to them as “high-temperature heat pumps” (HTHPs) [5]. These devices are employed in the industrial sector to recover waste heat and upgrade it to higher temperature streams directly supplying thermal processes. Examples of possible applications are drying processes, distillation and steam production [6]. High-temperature heat pumps have a great potential to produce process heat in the range between 100°C and 200°C. Industrial waste heat in Europe is estimated to be around 300 TWh/y and is typically available at temperatures lower than 100°C, while about 20% of the thermal energy demand has a temperature between 100-200°C [7]. Nevertheless, current state of the art HTHPs cannot reach temperatures above 150°C and have a maximum temperature lift of 100°C [8]. Therefore, the development of HTHPs which supply heat up to 200°C has a vital contribution for the transition towards a sustainable and renewables-based industry.

The development of HTHPs able to reach up to 200°C presents several challenges. One of the main barriers is represented by the development of compressors that can operate at temperatures close to 200°C. Compressors operating at this temperature level and beyond are currently being developed, but they are still in the research stage. So far, only five pilot scale demonstration projects, with thermal power lower than 0.1 MW and max temperature 160°C, are installed in the EU [9]. Another significant challenge is represented by the choice of the refrigerant. The latter should present high performance and be able to operate at high temperature, have a low global warming potential (GWP) and zero ozone depletion potential (ODP). Nowadays, hydrofluoroolefins (HFOs) are proposed as synthetic refrigerants for high-temperature applications. However, recent studies showed that HFOs produce trifluoroacetic acids when they decompose, which has potential destructive environmental effects [10]. Using natural refrigerants such as water, ammonia, CO_2 and hydrocarbons can be a valid alternative. However, these refrigerants have their own limitations. Ammonia and CO_2 require very high pressure levels when operating at high temperatures. Hydrocarbons are flammable, so there is a need for sophisticated safety measures against flammability and additional costs are generated when they are used as refrigerants. Water requires high pressure ratio and swept volume, which sometimes makes the systems inviable [11]. Therefore, finding an ideal refrigerant that satisfies all the requirements including thermal suitability, environmental compatibility, safety, efficiency and availability is still a major challenge for the development of HTHPs.

For conventional heat pumps, with the heat sink temperature lower than 100°C, it was shown that zeotropic mixtures could have a great potential as refrigerant. This is due to their non-isothermal phase change that can match the temperature profile of the heat sink and heat source, thus reducing the exergy destruction and improving the heat pump performance [12]. By proper selection of the components in the zeotropic mixture, it is also possible to reduce the GWP and flammability compared to pure fluids [13]. Moreover, it was demonstrated in the literature that high compression ratios and temperatures can be avoided through appropriate mixture selection [12]. However, studies on the application of zeotropic mixtures as working fluids in HTHPs are scarce. Zühlsdorf et al. [14] evaluated seven zeotropic mixtures composed of Propane, Iso-Butane, n-Butane and Iso-Pentane in a HTHP with the heat sink temperature at 130°C. The temperature glide in the source and sink was 25°C and 55°C, respectively. Based on their analysis, Propane/Iso-Pentane (50/50 wt%) resulted in the highest coefficient of performance (COP) of 3.08, while the highest COP for the pure fluids was 2.89. Bamigbetan et al. [15] compared the performance of zeotropic mixtures consisting of Propane, n-Butane, n-Pentane, and ammonia in three different heat pump configurations. The heat source inlet temperature was 40°C, and the heat sink outlet temperatures varied between 90°C and 150°C. The temperature glide in the heat sink and heat source was 10°C and 30°C, respectively. The authors found that a cascade system working with n-Butane/n-Pentane (40/60 wt%) resulted in the highest COP, which was around 13% higher compared to the COP of the best pure fluid. Zhang et al. [16] investigated several near-azeotropic mixtures composed of HFOs to substitute R-134a and R-114 in HTHPs. To do that, a heat pump model with a fixed temperature lift of 45°C and a variable condensing temperature in the range of 70°C - 110°C was employed. Results showed that compared to R-134a, the use of R1234zf/Propane (60/40 wt%) lead to 1.5% higher COP, with the HTHP operating at a lower compressor discharge temperature and a lower compression ratio. Guo et al. [17] studied potential zeotropic mixtures of hydrocarbons as refrigerants in a HTHP to heat up water from 15°C to 99°C. They concluded that a mixture of n-hexane/propene with the optimal mole fraction of 0.140/0.860 resulted in the highest COP. The authors also showed that the performance of this zeotropic mixture is better than transcritical cycles with CO_2 or CO_2 mixtures. Xu et al. [18] compared the performance of a binary mixture named HG-1 with three binary mixtures containing R245fa and with pure R245fa in a HTHP setup with a source temperature in the range of 80–100°C and a temperature lift of 40°C. Results showed that HG-1 is associated to the lowest exergy destruction and to the highest COP compared to the other working fluids.

On the basis of the review of the literature, it is clear that there is potential for zeotropic mixtures for high temperature heat pumps, even if the existing analyses consider only a few mixtures and there is not yet a clearly identified refrigerant for the different applications. While the benefits of zeotropic mixtures are recognized, the available studies are limited and case specific. Furthermore, previous works were always focused on applications with a sink temperature lower than 150°C. Therefore, the purpose of this work is to extend the range of the analysis in a systematic manner in order to identify zeotropic mixtures that can be used in HTHPs delivering heat up to 200°C, comparing their performance with pure fluids on the basis of the application considered. In previous studies, the analysis was done only on a few selected mixtures with a fixed composition. As such, it is essential to do a comprehensive analysis on different types of binary mixtures including natural refrigerants, hydrocarbons and HFOs with varying composition. The purpose is therefore to analyze a wide range of environmentally friendly binary mixtures (low GWP and ODP) to be used in HTHPs delivering heat in the range of 160°C to 200°C. Given the relevance of the integration of the high temperature heat pump within the process, on the basis of the most common industrial processes, three potential process archetypes have been identified with different temperature glides in the heat source and heat sink: latent/latent (e.g. distillation processes), latent/sensible (e.g. superheated steam drying), sensible/sensible (e.g. pressurized water production). A thermodynamic model coupled with an efficient optimization framework determines the optimum process parameters as well as the optimum composition for each of the binary mixtures. The mixtures are then compared in terms of COP, volumetric heating capacity (VHC), temperature glide and technical considerations like flammability of the refrigerants, compression ratio, compressor outlet temperature, and pressure levels at the evaporator and the condenser. The final aim is to provide guidelines to choose the best mixture for each process archetype.

2. Methods

In this section the methods used in the analysis are described. Firstly, the cycle architecture for the thermodynamic analysis is presented together with the optimization framework specifications. Secondly, three main industrial processes for the integration of high temperature heat pumps are described. Indeed, the process integration is paramount to assess the performance of a high temperature heat pump. For this reason some of the most promising processes, on the basis of the literature analysis, have been selected and used to define the boundary conditions for the cycle optimization: (i) distillation; (ii) superheated steam drying; (iii) pressurized hot water. Thus a more realistic assessment can be performed and useful indications for the most interesting applications for zeotropic mixtures can be drawn. Lastly, the selection of the fluids considered is presented.

2.1. Thermodynamic model of the heat pump cycle

Figure 1 shows an overview of the HTHP cycle and the corresponding TH diagram. The main components are: the evaporator and condenser, the internal heat exchanger (IHX), the compressor and the thermal expansion valve (TXV). After leaving the evaporator (state 1), the refrigerant is superheated in the IHX to state 2. It is subsequently compressed to state 3 and then cooled in the condenser to state 4, delivering high-temperature process heat. The refrigerant is further cooled down in the IHX to state 5 and then expands through the TXV to state 6. Finally, the refrigerant enters the evaporator where it absorbs heat from a low-grade waste heat source.

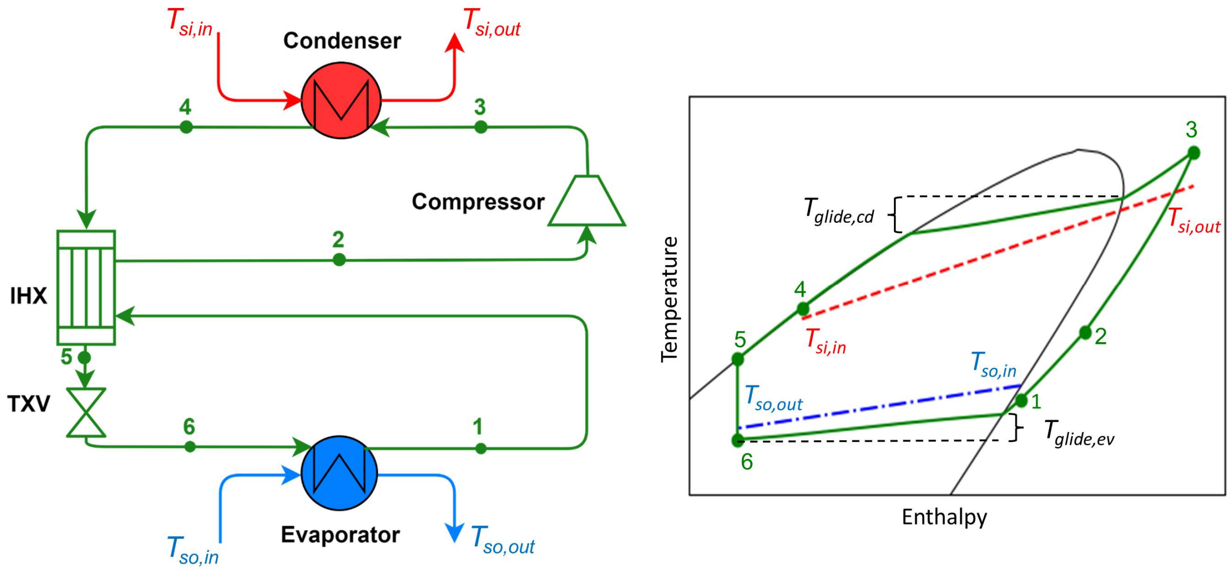

Figure 1. Overview of a HTHP cycle and its corresponding TH diagram.

The HTHP is modelled under the following assumptions:

1. The system operates under steady-state conditions;

2. The heat loss in the system components and piping is negligible;

3. The pressure drop in the heat exchangers and piping is negligible [17];

4. The compressor operates with a fixed isentropic efficiency (η_{is}) of 0.75. Although the isentropic efficiency is fluid dependent [19], a fixed efficiency is used for the first assessment due to the large amount of fluids screened and to favor a fair comparison.

5. The expansion in the TXV is isenthalpic;

6. The IHX has a fixed effectiveness of either $\epsilon = 0.75$ or $\epsilon = 0$ if a case with no IHX is simulated. The effectiveness is defined as the ratio of the actual heat transfer to the maximum possible heat transfer in the IHX [20].

In order to uniquely determine the thermodynamic states of the HTHP cycle, several parameters need to be specified. Firstly the boundary conditions about the heat sink and source need to be known and they depend on the considered industrial process. As for the heat sink, the mass flow rate and the inlet and outlet states are defined by the process into which the HTHP is integrated:

1. Inlet state of the heat sink: pressure (p_{si}), temperature ($T_{si,in}$) or vapor quality ($q_{si,in}$) when in two phase region;

2. Outlet state of the heat sink: temperature ($T_{si,out}$) or vapor quality ($q_{si,out}$) when in two phase region;

3. Mass flow rate of the heat sink ($\dot{m}_{si}$).

Similar parameters are defined for the heat source. However, the outlet state is linked to the amount of heat extracted by the heat sink and the performance of the heat pump. Hence, only the inlet state of the heat source is given as input:

4. Inlet state of the heat source: pressure (p_{so}), temperature ($T_{so,in}$) or vapor quality ($q_{so,in}$) when in two phase region;
5. Mass flow rate of the heat source ($\dot{m}_{so}$).

Given the relevance of the boundary conditions for the thermodynamic analysis, some relevant case studies have been selected and they are further discussed in section 2.3. The cycle variables that characterize the thermodynamic behavior of the system (i.e. objective function) are:

1. Pressure at the evaporator (p_{ev});
2. Pressure at the condenser (p_{cd});
3. Degree of superheating in the evaporator (ΔT_{sh});
4. Degree of subcooling in the condenser (ΔT_{sc});
5. Composition of the binary refrigerant used as the working fluid (z_{mole}).

For a subcritical cycle, where the condenser and the evaporator are operating at a pressure lower than the critical pressure of the refrigerant, the subcooling ΔT_{sc} is defined as the difference between the temperature at the saturated liquid state at p_{cd} and the condenser outlet temperature. Similarly, the superheating ΔT_{sh} is defined as the difference between the evaporator outlet temperature and the saturated vapor state at p_{ev}, which is always positive. For transcritical cycles, the definition for ΔT_{sc} cannot be used as there is no saturation temperature for pressures above the critical point. Therefore, for those cases, ΔT_{sc} is defined as the difference between the critical temperature and the condenser outlet temperature, which can be either positive or negative.

By providing the discussed input parameters (i.e. boundary conditions and cycle variables), the heat pump cycle can be evaluated and the mass flow rate of the refrigerant and its state in different points of the cycle (points 1 to 6 in Figure 1) can be determined. The calculations are done in Python. The REFPROP 10.0 database [21] is accessed in the code for determining the thermodynamic properties of the working fluid and secondary fluids in the cycle.

Once all the cycle states are known, the energetic performance of the heat pump is assessed using the COP: this is the ratio of the useful heat delivered to the heat sink over the compressor work. The COP and VHC can be calculated with Equation 1 and 2, respectively.

$$COP = \frac{h_3 - h_4}{h_3 - h_2} \tag{1}$$

$$VHC = \frac{h_3 - h_4}{\rho_2} \tag{2}$$

Here h and ρ represent the enthalpy and density (at the compressor inlet) of the working fluid, respectively.

Once the cycle is simulated, the minimum temperature approach at both evaporator and condenser (MTA_{ev} and MTA_{cd}, respectively) can also be determined. The minimum temperature approach is defined as the minimum temperature between the refrigerant and the secondary fluid in a heat exchanger. These parameters are essential for designing the heat exchangers, as they directly affect the required heat transfer area and hence the cost.

2.2. Optimization strategy

An optimization framework was developed to find the maximum achievable COP for each binary mixture at given boundary conditions. The model optimizes five cycle parameters discussed in section 2.1: ΔT_{sh}, ΔT_{sc}, p_{ev}, p_{cd}, and z_{mole} of the binary mixture. The optimization is done for two HTHP cycle configurations: a cycle with IHX and a cycle without IHX. In this way, an optimal cycle configuration is found for each selected mixture, both with and without IHX. This allows a better understanding of the influence of an IHX on the cycle performance.

The overview of the optimization framework is shown in Figure 2. The basin-hopping global optimizer implemented in SciPy library in Python [22] is used as the optimization algorithm. Three soft constraints are considered in the optimization framework. The first two constraints impose a minimum value for the MTA in the condenser and evaporator: MTA_{ev} and MTA_{cd} have to be greater than 5 K. The optimizer would indeed tend to reach a zero MTA to maximize the COP, which is technically not possible. The minimum MTA of 5 K gives a suitable trade-off between thermal and economic performance [23]. The third constraint is set to avoid wet compression. The three constraints are implemented as soft constraints, i.e. if a constraint is not met, a penalty is applied to the objective function (COP). No constraints are considered on the compressor outlet temperatures, compression ratios and pressure levels at the evaporator and condenser. These aspects are analyzed afterwards and discussed in the results section.

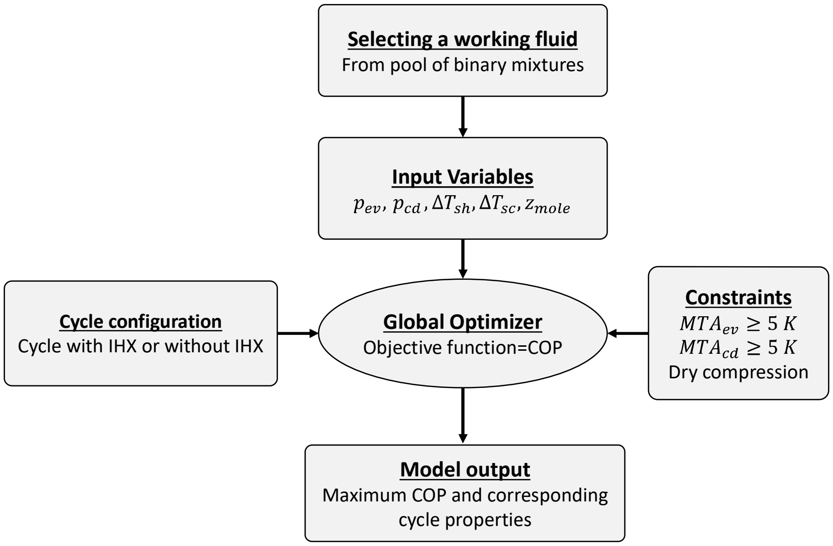

Figure 2. Overview of the optimization framework used to optimize the HTHP cycle.

2.3. Identified cases for the integration of heat pumps

Three generic industrial cases for the integration of HTHPs are identified. These cases are obtained from literature and from bilateral meetings with several chemical companies in Flanders, Belgium. Each case is described in detail below. The general specifications of the heat sink and heat source of these case studies are summarized in Table 1. Thanks to these cases it is possible to perform a more specific analysis with real boundary conditions and to determine in which applications high temperature heat pumps with zeotropic mixtures achieve competitive results.

Table 1. General specification of the heat sink and heat source for the selected processes for integration of a HTHP.

Process	Lorenz COP	Reference	Heat Source					Heat Sink				
			Fluid	$\dot{m}$ [kg/s]	T_{in} [°C]	T_{out} [°C]	p [bar]	Fluid	$\dot{m}$ [kg/s]	T_{in} [°C]	T_{out} [°C]	p [bar]
Distillation	6.76	[24]	99.5% B 0.5% T	17.5	97.3	97.2	1.65	93.6% EB 6.4% T	26.56	161.2	162	2
Superheated Steam Drying (SSD)	8.95	[25]	Steam	0.13	115	99.83	1.008	Steam	2.27	116	197	1.008
Pressurized hot water production (PHWP)	6.37	Interview with companies	Water	70	110	---	3	Water	30	140	200	55

B: Benzene, T: Toluene, EB: Ethylbenzene, EG: Ethylene glycol

2.3.1. Case 1 – distillation

Distillation is a common separation method in chemical industries, which also accounts for a large energy use in chemical industries [24]. The integration of a heat pump in a distillation column can reduce the energy consumption significantly. So far, different types of distillation columns are developed and used in industrial sectors. In the present study, a dividing-wall column (DWC), which allows for separating multi-component mixtures (e.g. tertiary mixtures), is studied for integration of a HTHP [25,26]. This specific case study is based on the work of Chew et al. [24] who used a DWC for separation of Toluene (T), Ethylbenzene (EB) and Ethylene glycol (EG). The HTHP can be integrated into this process by recovering heat from the condenser, upgrading it, and delivering it to the reboiler (Figure 3). Therefore, the output stream on the top of the tower is the heat source, and the outlet stream on the bottom of the tower is the heat sink for the HTHP. The properties for these two streams are reported in Table 1. The heat source is not pure benzene, so there is a slight temperature glide from 97.3°C to 97.2°C in the condenser of the DWC. In the same way, the heat sink temperature slightly varies from 161.2°C to 162°C in the reboiler. Hence, this process requires a temperature lift of around 64°C.

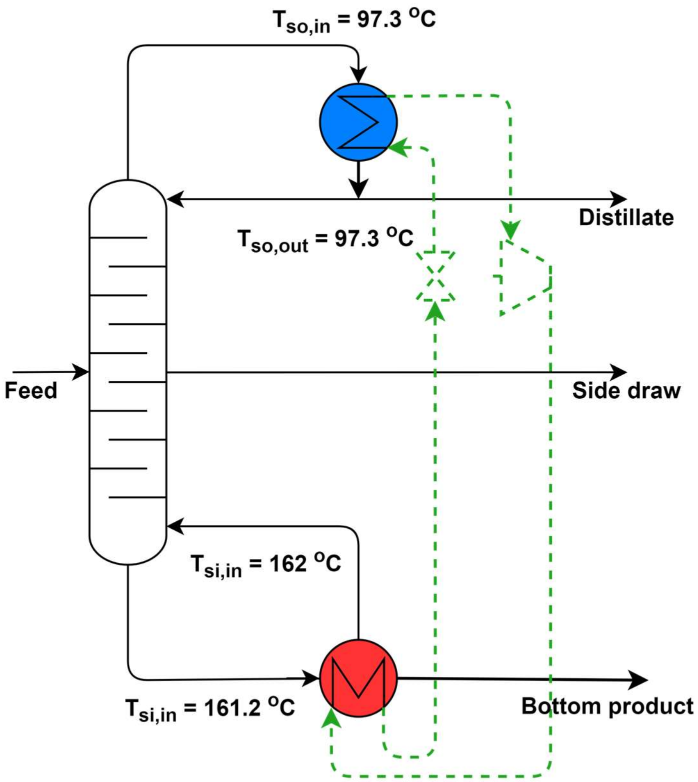

Figure 3. Integration of HTHP in DWC process [24] for distillation of benzene, toluene and ethyl benzene.

2.3.2. Case 2 – Superheated Steam Drying

Superheated steam drying (SSD) is an innovative drying technology, utilizing superheated steam as a drying medium to remove excess water from a wet material [27]. Bang-Möller et al. [28] introduced a combined heat and power plant for biomass conversion. The first process that this plant deals with is the drying of wet biomass (42% water) by means of a SSD, which is the relevant process for integrating a HTHP (Figure 4). In the process suggested by Bang-Möller et al. [28], the superheated steam acts both as heat source and as drying medium to take away the evaporated water. The evaporated water represents the excess superheated steam recirculated to the heat source. Furthermore it is assumed that all the steam can be recuperated from the dried product, which should be possible if air infiltration is avoided [29].

The excess steam is firstly cooled from 115°C to its saturation temperature (100°C) and is then condensed to a saturated liquid state (100°C), supplying heat to the HTHP. Note that the resulting heat transfer is mainly latent, hence the temperature difference in the source does not result in a temperature glide of 15°C throughout the whole heat exchanger. The extracted heat is then upgraded by the HTHP and transferred to the superheated drying steam, i.e. the heat sink, increasing its temperature from 115°C to 197°C, resulting in a temperature glide of 82°C in the heat sink. The corresponding properties of the heat sink and heat source for this case study are reported in Table 1.

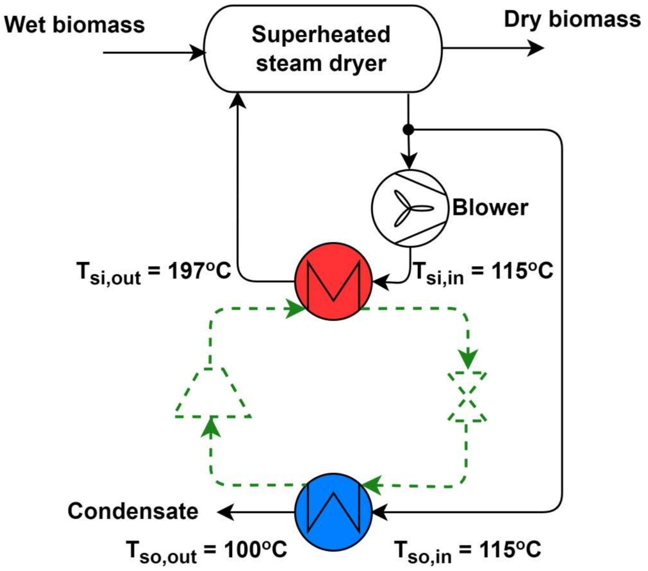

Figure 4. Integration of HTHP in superheated steam dryer [28] for drying of wet wood.

2.3.3. Case 3 – Pressurized Hot Water Production

Many industrial sectors, e.g., pharma and food industry, use pressurized hot water for heat supply in their processes. Hot water streams are typically produced by means of a boiler which burns natural gas or other fossil fuels [30]. After delivering heat to different units, the stream of hot water returns to the boiler at a lower temperature and is heated up again to circulate in the process. HTHPs can be used to heat the pressurized hot water system and thereby substitute the boiler (Figure 5). For the integration of a HTHP in this process, a heat source is required which can be both internal or external to the process itself [31]. Therefore, the use of a HTHP instead of a boiler can also help to reduce the loads to the cooling system, increasing the overall efficiency of the industrial site.

The boundary conditions of this case study were obtained by interviewing several companies in Flanders, Belgium. The data obtained from these interviews were aggregated and generalized to have a representative process. In this generalized case, the heat sink is pressurized water at 55 bar, which is heated from 140°C to 200°C. The heat source is a hot water waste stream at a temperature of 110°C and a pressure of 3 bar. The main specifications of the heat sink and heat source streams are reported in Table 1.

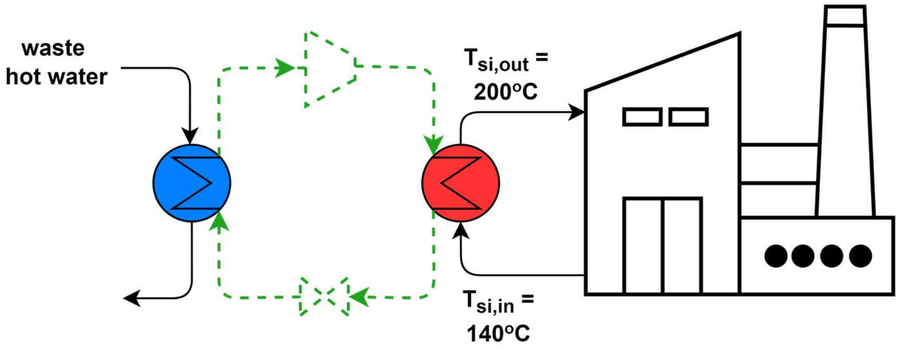

Figure 5. Using HTHP for production of pressurized hot water.

2.4. Screening of binary mixtures

In order to select the binary mixtures for this analysis, the pure fluids present in the REFPROP 10.0 database were considered. To restrict the analysis to a reasonable group of mixtures, three screening steps were performed. In a first step, all fluids with ODP higher than 0.0005 and GWP higher than 150 were discarded. The threshold value for GWP is based on the EU Regulation No. 517/2014 for refrigerants [32]. SO_2 was also removed from the list because of its unfavorable environmental effects. As for the second step of screening, the fluids with a critical temperature lower than 150°C or higher than 350°C were discarded. These assumptions were introduced to avoid mixtures with too different critical temperatures, because this results in unstable mixtures. Furthermore, the lower bound is aimed to favor subcritical cycles for the purpose of this analysis, while the upper bound eliminates fluids that would result in too low pressures in the evaporator. The last step consists of a post-processing to include any missing refrigerants which performed well in a preliminary heat pump optimization with pure fluids or other popular refrigerants for high-temperature applications, such as R1234yf, R1234ze(E), R1243zf, R161, R41, water, ammonia, CO_2, ethylene glycol, ethanolamine, O-xylene, which were added.

The proposed screening reduced the number of pure fluids from 144 to 55, which are listed in Appendix. This corresponds to 1346 binary mixtures to be analyzed for HTHP applications. While several binary mixtures are omitted from the list due to their environmental properties (GWP and ODP), no mixtures were eliminated because of their safety issues, as the term 'safe to operate' is hard to define in this case. However, for each working fluid, an indication is given based on ASHRAE 34 (American Society of Heating, Refrigerating and Air-Conditioning Engineers- [33]). The ASHRAE 34 standard is not available for all the screened pure fluids. In such case, NFPA 704 (U.S. National Fire Protection Agency [34]) is considered. NFPA 704 quantifies the toxicity, flammability and stability of substances on a scale between 0 to 4 (i.e. 5 grades). These grades are provided for the relevant fluids in the appendix.

It should be noted that the difference between the normal boiling point of the constituent components (ΔT_b) could also be considered as a constraint to limit the number of mixtures, since a large difference increases the chance of fractionation [35]. For example, Chys et al. [36] bounded the maximum normal boiling point difference to 45°C [36]. However, in the present study, no limitation is considered on the normal boiling point difference of the compounds of the mixtures, as the risk of fractionation is discussed afterwards for the best performing mixtures, as explained in section 2.5.

2.5. Risk for fractionation of binary mixtures

A mixture is called fractionated when in the two-phase region the vapor phase mostly consists of the more volatile components, and the liquid phase is mainly composed of the other components. In heat pump cycles, fractionation might take place in the evaporator or the condenser, where the mixture is in the two-phase region (Figure 6).

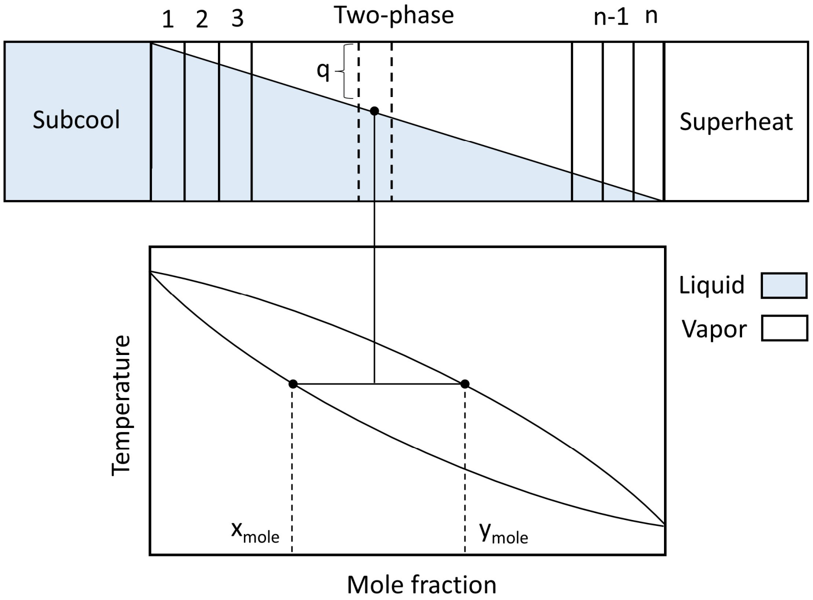

Figure 6. Fractionation of a zeotropic mixture in the evaporator and the condenser of the heat pump cycle.

In the presence of a leakage, undesired fractionation can cause a rapid composition shift in the refrigerant mixture and reduce the cycle performance [36]. In the present work, the risk of fractionation is analyzed by calculating the relative volatility (α). α is a measure of the ease or difficulty of separation of a given mixture to its constitute components by means of evaporation. For a binary mixture in the two-phase region, α can be calculated as follows:

$$\alpha = \frac{y_{\mathrm{mole}}(1 - x_{\mathrm{mole}})}{x_{\mathrm{mole}}(1 - y_{\mathrm{mole}})} \tag{3}$$

where x_{mole} and y_{mole} are the mole fraction of the more volatile compound in the equilibrium liquid and vapor phase, respectively. Large variations in α during evaporation and condensation of a mixture show that the tendency of separation varies, so there is a risk for fractionation. Therefore, in the present study, variation of α versus vapor quality (q) in the evaporator and condenser is considered as an indication for possible fractionation. It should be noted that there is no threshold for α to avoid fractionation and it is just a relative value showing the tendency of fractionation of different mixtures with respect to each other.

3. Results and Discussion

In this section the optimization results for the three considered applications for a HTHP with and without IHX are reported. The best performing mixtures are discussed in terms of cycle performance and other operational parameters, such as VHC, compression ratio and flammability issues, in order to provide guidelines for an informed choice of the most suitable refrigerants. All the results obtained are reported in the Supplementary material.

3.1. Optimization results for case 1: distillation

Heat pump without internal heat exchanger

For the distillation case, as expected, it was observed that the mole fraction for many of the mixtures was approximately 0 or 1. This means that these mixtures consist in essence of a single compound, i.e. they are pure fluids. Consequently, these mixtures have the same COP and properties as the corresponding pure fluids. This is due to the small temperature glide in the heat sink and the heat source. These results are not reported here, but readers can find the simulation results for all the screened mixtures in the Supplementary material. There were a few exceptions where binary mixtures provided a higher COP compared to the pure fluids. Water/heptane and water/toluene mixtures are among those exceptions. The optimized cycle properties for these near-azeotropic mixtures are compared with the pure constituent fluids in Table 2. The COP obtained by these mixtures is 4.05, which is slightly higher than for pure water (3.93). However, the VHC of these mixtures is lower compared to water. The temperature glides in the evaporator and the condenser are rather small, which means that both these mixtures are near-azeotropic. The TH diagrams of the HTHP working with water/toluene and pure water are compared in Figure 7. According to this figure, the compressor outlet temperature (point 3 in the figure) for water/heptane is 214°C, which is significantly lower compared to pure water (430°C). Therefore water/heptane has a better temperature match with the heat sink in the condenser, which is among the reasons for a higher COP compared to pure water. The reduction in the compressor outlet temperature is also beneficial for the operation of the heat pump, since regular compressors cannot operate at such high temperatures and there is a need for a cooling method to reduce the temperatures at the outlet of the compressor. According to the results of Table 2, binary mixtures also provide some advantages for the compressor in terms of compression ratio reduction. For water/heptane, the compression ratio is 8.6, which is lower than the compression ratio of pure water (9.7). These results indicate that the benefits of using binary mixtures as refrigerant is not limited to matching the temperature with the heat sink and heat source, but they can also improve the cycle by reducing the compression ratio and the compressor outlet temperature.

Table 2. Optimized cycle properties of selected mixtures and their constituent compounds in the HTHP without IHX, integrated into the distillation process.

fluid	p_{ev} [bar]	p_{cd} [bar]	$\frac{p_{cd}}{p_{ev}}$	ΔT_{sh} [°C]	ΔT_{sc} [°C]	z_{mole}	COP	VHC [kJ/m^3]	$T_{c,out}$ [°C]	$T_{glide,cd}$ [°C]	$T_{glide,ev}$ [°C]
Water/heptane	0.58	5.3	9.2	0.0	0.0	0.22	4.05	783	228	3.5	0.4
Water/toluene	0.54	4.7	8.6	0.0	0.0	0.42	4.05	701	214	2.6	0.2
Water	0.75	7.3	9.7	0.0	0.7	1	3.93	1193	430	0.0	0.0
Heptane	0.19	5.3	28.6	42.4	0.8	1	1.91	162	167	0.0	0.0
Toluene	0.41	4.0	9.7	10.4	0.7	1	3.16	406	167	0.0	0.0

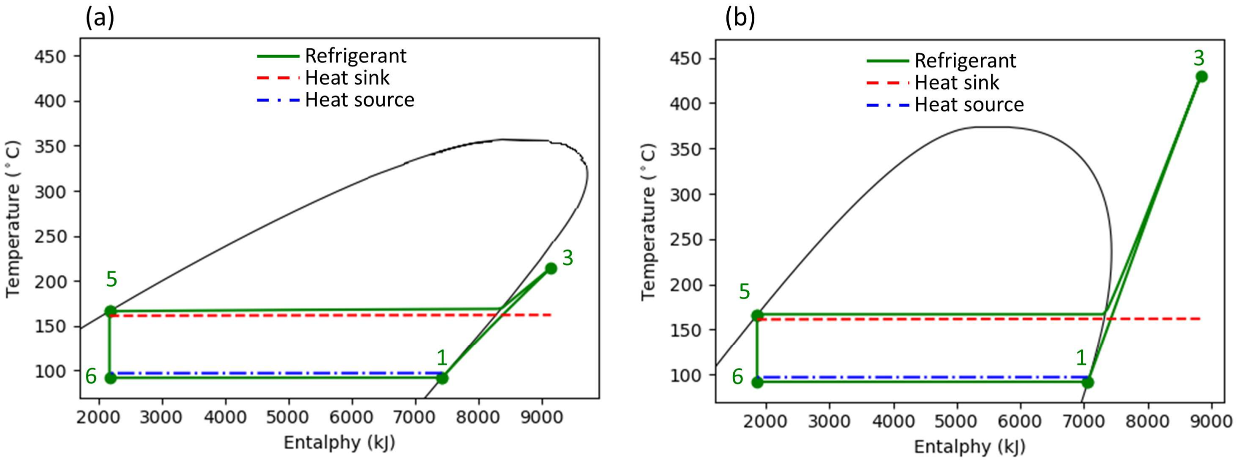

Figure 7. TH diagrams of the HTHP cycle without IHX integrated into the distillation case for (a) water/toluene mixture and (b) pure water as refrigerant.

Heat pump with internal heat exchanger

Similarly to the case without IHX, it was observed that most of the best performing mixtures consist of only one compound. This is again due to the small temperature change in the heat sink and heat source. Also in this case water/toluene and water/heptane mixtures resulted in a higher COP compared to pure water (Table 3). Temperature glides of these mixtures are quite small, but compared to the pure fluids, they allow a higher COP. They also reduce the compression ratio and outlet temperature of the compressor, compared to pure water. Apart from these advantages, their VHCs were lower compared to the VHC of pure water.

Table 3. Optimized cycle properties of selected mixtures and their constituent compounds in the HTHP with IHX, integrated into the distillation process.

fluid	p_{ev} [bar]	p_{cd} [bar]	$\frac{p_{cd}}{p_{ev}}$	ΔT_{sh} [°C]	ΔT_{sc} [°C]	z_{mole}	COP	VHC [kJ/m^3]	$T_{c,out}$ [°C]	$T_{glide,cd}$ [°C]	$T_{glide,ev}$ [°C]
Water/heptane	0.54	4.2	7.7	0.0	0.0	0.64	4.11	711	241	0.7	0.0
Water/toluene	0.57	4.7	8.2	0.0	0.1	0.38	4.11	643	246	0.6	0.1
Water	0.75	7.3	9.7	0.0	0.0	0	3.67	791	531	0.0	0.0
Heptane	0.58	4.0	6.9	0.0	0.7	0	4.06	1111	212	0.0	0.0
Toluene	0.83	5.3	6.4	0.1	0.7	1	3.86	622	192	0.0	0.0

It should be kept in mind that toluene and heptane are not miscible with water, so using them as refrigerant in the heat pump cycle could be problematic. Moreover, water/toluene and water/heptane are flammable mixtures. Thus, their use requires several additional safety measures compared to pure water. Overall, by considering all the advantages and challenges, for the cases with constant/small temperature variation in heat sink and heat source, binary mixtures do not provide a significant added value compared to the pure fluids. Therefore, binary mixtures are not suggested as the refrigerant for these cases.

3.2. Optimization results for case 2: Superheated steam drying

Heat pump without internal heat exchanger

For the SSD case, where there is a temperature difference mainly in the heat sink (15.17°C and 81°C in the heat source and heat sink, respectively), the optimum mole fraction for many of the mixtures is again 1 or 0, meaning that these mixtures contain only one component. Like for the distillation case, there are few exceptions where binary mixtures resulted in a higher COP compared to the pure fluids. As an example, cycle properties for cyclobutene/R1234ze(Z) and their constituent compounds are reported in Table 4. The COP obtained with this mixture is 4.12, which is slightly higher than the COP of pure cyclobutene (4.11).

Table 4. Optimized cycle properties of a selected mixture and its constituent compounds in the HTHP without IHX, integrated into the SSD process.

fluid	p_{ev} [bar]	p_{cd} [bar]	$\frac{p_{cd}}{p_{ev}}$	ΔT_{sh} [°C]	ΔT_{sc} [°C]	z_{mole}	COP	VHC [kJ/m^3]	$T_{c,out}$ [°C]	$T_{glide,cd}$ [°C]	$T_{glide,ev}$ [°C]
R1234ze(Z)/cyclobutene	13.2	60.9	4.6	2.1	52.4	0.06	4.12	10104	202	0.0	0.1
R1234ze(Z)	11.6	71.1	6.1	3.1	29.1	1.00	3.88	8871	202	0.0	0.0
Cyclobutene	13.1	60.7	4.6	0.0	53.9	1.00	4.11	10071	202	0.0	0.0

To investigate these results in more detail, the TH diagrams of the heat pump cycle for cyclobutene/R1234ze(Z) and pure cyclobutene are shown in Figure 8. While there is a difference in the inlet and outlet temperature of the heat source, the source temperature suddenly drops to the saturated temperature and afterward remains constant. Therefore, the heat source does not have a constant temperature glide, like the heat sink. This is because the heat source is superheated water close to the saturation conditions. As a result, the heat source behaves mainly as a latent heat source, although there is a difference in its inlet and outlet temperature. On the other hand, the heat sink is sensible with a large temperature glide. Therefore, an ideal refrigerant for this case should have a constant temperature profile in the evaporator and a large temperature glide in the condenser. Since zeotropic mixtures have a temperature glide both in the evaporator and the condenser, they do not result in a higher COP compared to pure fluids or near-azeotropic mixtures. Transcritical cycles can provide a high-temperature glide at the condenser and a constant temperature at the evaporator. Therefore, they could be an excellent choice for the HTHP integrated in the SSD process. This is the case for cyclobutene/R1234ze(Z) and cyclobutene as shown in Figure 8. It should be noted that most of the best performing refrigerants for this case study are indeed transcritical. Readers can refer to the supplementary file for more information.

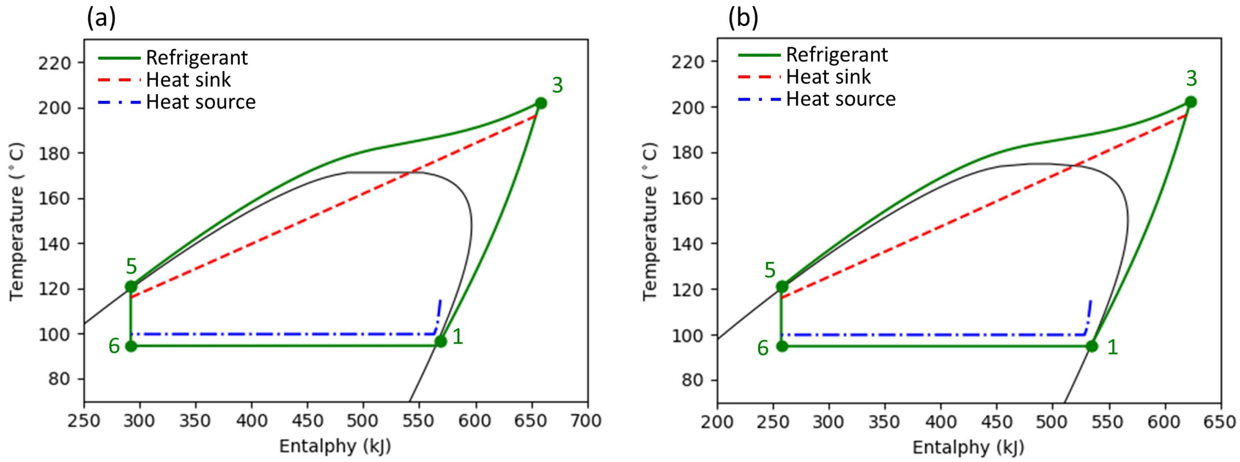

Figure 8. TH diagrams of the HTHP cycle without IHX integrated into the SSD case for (a) cyclobutene/R1234ze(Z) mixture and (b) pure cyclobutene as refrigerant.

Heat pump with internal heat exchanger

Based on the optimization results, the COP of the HTHP cycle with IHX is slightly higher than the COP of the cycle without IHX. The best performing mixtures are also different for the two configurations. However, just like the case without IHX, the optimized composition of these mixtures is very close to 0 or 1, meaning that they are pure fluids and not a binary mixture. Most of the best performing refrigerants are transcritical, like the case without IHX. There were some exceptions where binary mixtures performed better than the pure fluids, but the difference between their COP is very small. As an example, the cycle properties of a R1234ze(Z)/cyclobutene mixture and its constituent compounds are reported in Table 5. The temperature glide of this mixture both in the evaporator and the condenser is zero, meaning that the mixture is azeotropic. The optimized COP of the cycle for this mixture is 4.32, which is very close to the COP obtained by pure R1234ze(Z) (4.31). The VHC of R1234ze(Z)/cyclobutene is slightly higher than VHC of Cyclobutene and R1234ze(Z). These results indicate that the use of a zeotropic mixture does not lead to a higher COP if the temperature glide is present solely in the heat sink and not in the heat source. However, they can provide some improvements in reducing the compression ratio and compressor outlet temperature.

Table 5. Optimized cycle properties of a selected mixture and its constituent compounds in the HTHP with an IHX, integrated into the SSD process.

fluid	p_{ev} [bar]	p_{cd} [bar]	$\frac{p_{cd}}{p_{ev}}$	ΔT_{sh} [°C]	ΔT_{sc} [°C]	z_{mole}	COP	VHC [kJ/m^3]	$T_{c,out}$ [°C]	$T_{glide,cd}$ [°C]	$T_{glide,ev}$ [°C]
R1234ze(Z)/cyclobutene	13.7	56.9	4.1	1.9	46.3	0.70	4.32	10422	204	0.0	0.0
R1234ze(Z)	6.2	43.2	6.9	1	50	---	4.31	9498	202	0.0	0.0
Cyclobutene	13.12	54.3	4.1	2.3	53.9	---	4.29	10204	208	0.0	0.0

3.3. Optimization results for case 3: Pressurized hot water production

Heat pump without internal heat exchanger

For the PHWP case, the temperature glide is present both in the heat sink and heat source, therefore zeotropic mixtures can result in a good match with these temperature profiles, leading to a higher COP compared to their constituent pure components. The results confirm this. The cycle properties for some of the best performing mixtures, and for their pure compounds for reference, are reported in Table 6. Ethanol/p-Xylene and ethylbenzene/methanol resulted in the highest COP of 3.60. This is around 10 % higher than the highest COP of the pure fluids, which is 3.28 obtained by methanol. Such an improvement in COP is comparable to the outcomes of other works [14-18]. Apart from a higher COP, zeotropic mixtures resulted in lower compression ratios and lower compressor outlet temperatures compared to pure fluids. The compression ratio associated to pure ethanol is 18.5, which is reduced to 12.8 with the ethanol/p-Xylene mixture. Moreover, the compressor outlet temperature of 254°C for pure ethanol was reduced to 217°C for ethanol/p-Xylene mixture. However, for this mixture the VHC decreased. The VHC of some zeotropic mixtures such as water/acetone and water/ammonia was equal or higher than the VHC of their constituent compounds, while for others it was lower, overall there was not a clear trend for this variable.

Table 6. Optimized cycle properties of selected mixtures and their constituent compounds in the HTHP without IHX, integrated into the PHWP process.

fluid	p_{ev} [bar]	p_{cd} [bar]	$\frac{p_{cd}}{p_{ev}}$	ΔT_{sh} [°C]	ΔT_{sc} [°C]	z_{mole}	COP	VHC [kJ/m^3]	$T_{c,out}$ [°C]	$T_{glide,cd}$ [°C]	$T_{glide,ev}$ [°C]
ethanol/p-Xylene	1.1	14.6	12.8	0	32	0.68	3.60	1469	217	26.8	19.2
methanol/ethyl benzene	2.0	21.4	10.7	0	31	0.80	3.60	2509	248	19.5	19.2
toluene/ethanol	1.2	14.2	11.5	3	33	0.60	3.57	1472	207	27.9	15.4
methanol/m-Xylene	2.0	22.9	11.3	3	33	0.84	3.54	2607	259	14.2	16.3
water/ethanol	1.1	16.7	14.9	1	34	0.76	3.51	1805	378	12.2	9.8
water/acetone	1.9	20.2	10.6	2	34	0.57	3.50	2432	289	7.0	20.6
water/ammonia	1.3	15.8	12.5	0	0	0.79	3.48	1112	473	45.5	24.3
R1234ze(Z)/acetone	5.8	41.1	7.0	8	43	0.55	3.22	4568	210	0.0	8.7
R1234ze(Z)/benzene	6.5	43.9	6.7	0	41	0.74	3.19	4748	207	0.0	18.6
methanol	2.3	31.5	13.8	0	31	---	3.28	3108	289	0.0	0.0
toluene	0.4	8.0	21.7	26	30	---	2.55	336	208	0.0	0.0
ethanol	1.4	25.9	18.5	0	36	---	3.18	1946	231	0.0	0.0
water	0.6	12.2	19.4	1	29	---	3.10	1112	232	0.0	0.0
acetone	2.5	24.5	9.8	20	31	---	2.98	2192	254	0.0	0.0

Most of the best performing mixtures, including ethanol/p-Xylene, are highly toxic and flammable. Therefore, using these mixtures as a refrigerant in the HTHP cycle can be an issue. Water/ethanol and water/acetone are two options with lower toxicity and flammability and a higher COP compared to the methanol (COP of 3.51 and 3.50 for water/ethanol and water/acetone, respectively). The best mildly-flammable mixture in terms of COP is water/ammonia, which resulted in a COP of 3.48. This is 12% higher than the COP of pure water (3.01). While the concentration of ammonia in this mixture is rather small, special care need to be taken due to the toxicity of ammonia. The other issue with this mixture is the high-temperature at the compressor outlet compared to other mixtures. However, the compressor outlet temperature for water/ammonia is lower than that of pure water (Figure 9). Moreover, this problem is solvable at a certain cost by means of intercooling between different compression stages or liquid injection during the compression [37, 38]. Other non-flammable/mildly flammable mixtures (mixtures of HFOs and CO_2) did not perform well, they resulted in a lower COP compared to their constituent compounds. The results for those mixtures are provided in the Supplementary material.

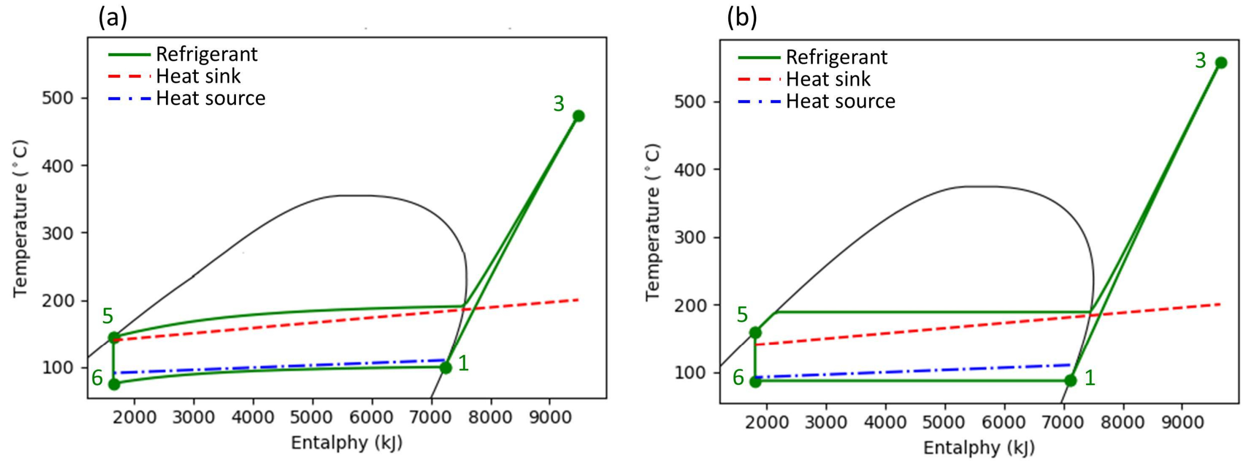

Figure 9. TH diagrams of the HTHP cycle without IHX integrated into the PHWP case for (a) water/ammonia and (b) water as refrigerant.

Mixtures of a HFO and a hydrocarbon can also be an option with lower flammability compared to a pure hydrocarbon. The best performing mixtures of such kind are R1234ze(Z)/acetone and R1234ze(Z)/benzene with COP of 3.22 and 3.19, respectively. While the COP of these mixtures is lower than the mixtures of hydrocarbons, they still resulted in a higher COP compared to their constituent components. The cycle for the previous mixtures was subcritical, whereas the cycle for R1234ze(Z)/acetone and R1234ze(Z)/benzene is transcritical, due to their lower critical temperature. As an example, the TH diagram of the HTHP cycle for the ethanol/p-Xylene mixture is compared with the one of R1234ze(Z)/benzene in Figure 10. There is a temperature glide both during evaporation and condensation of ethanol/p-Xylene, but there is a better temperature matching in the evaporator rather than in the condenser. The temperature glide of ethanol/p-Xylene in the condenser is 26.8°C, which is lower than the temperature glide of the heat sink (60°C). Therefore, a 32°C of subcooling contributed to improve the temperature matching in the condenser. For R1234ze(Z)/benzene mixture, there is a temperature glide in the evaporation process which perfectly matches the temperature glide of the heat source. The operating pressure of the condenser (gas cooler) is higher than the critical pressure of R1234ze(Z)/benzene and heat is released with a temperature glide that matches the temperature profile of the heat sink.

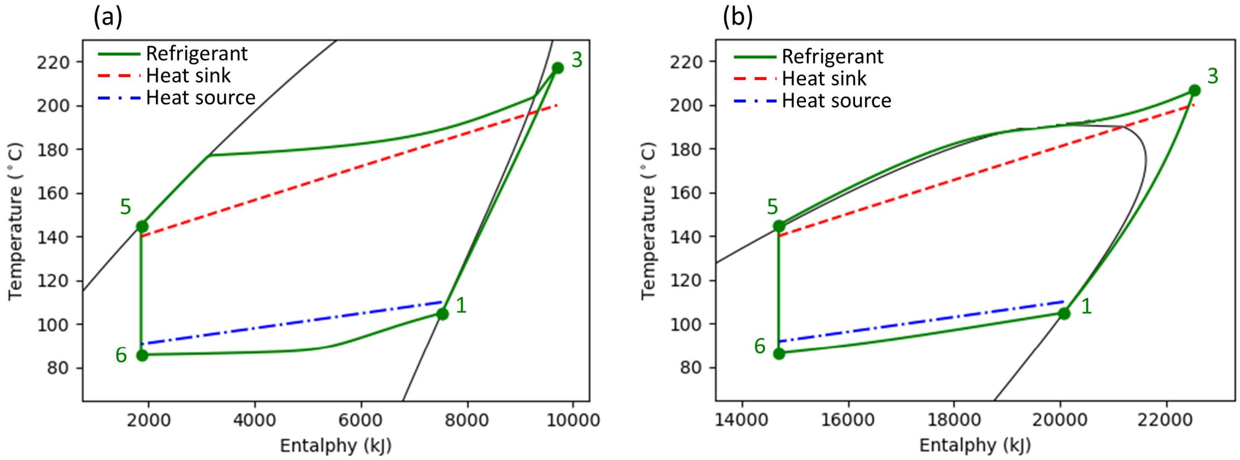

Figure 10. TH diagrams of the HTHP cycle without IHX integrated into the PHWP case for (a) ethanol/p-Xylene and (b) R1234ze(Z)/benzene as refrigerant.

Heat pump with internal heat exchanger

The cycle properties for some of the most interesting studied mixtures for this case are reported in Table 7. The maximum achieved COP was 3.89 (achieved by toluene/ethanol) which is higher than the maximum COP for the case with no IHX (3.60 obtained by ethanol/p-xylene). While the best performing mixtures are quite different from the case without IHX, on average, the COPs are higher than the case without IHX. Just like the case without an IHX, higher COPs are obtained by using the mixtures rather than pure fluids. The highest COP given by the pure fluids was 3.38 (for cyclobutene) which is significantly lower than the highest COP for binary mixtures. Moreover, binary mixtures are characterized by a lower compression ratio and compressor outlet temperatures compared to pure fluids (see, for example, the results for toluene/ethanol and pure toluene).

Table 7. Optimized cycle properties of selected mixtures and their constituent compounds in the HTHP with an IHX, integrated into the PHWP process.

fluid	p_{ev} [bar]	p_{cd} [bar]	$\frac{p_{cd}}{p_{ev}}$	ΔT_{sh} [°C]	ΔT_{sc} [°C]	z_{mole}	COP	VHC [kJ/m^3]	$T_{c,out}$ [°C]	$T_{glide,cd}$ [°C]	$T_{glide,ev}$ [°C]
toluene/ethanol	1.2	11.1	9.5	0	24	0.67	3.89	1416	224	30.2	17.8
cyclohexane/methanol	2.9	21.4	7.4	3	24	0.65	3.81	2927	221	26.8	16.8
benzene/m-xylene	0.7	7.2	10.8	0	39	0.56	3.75	815	216	17.6	18.4
methanol/ethyl benzene	2.0	19.9	10.0	0	28	0.80	3.67	2463	276	19.9	19.5
water/acetone	2.2	20.2	9.3	0	39	0.48	3.64	2666	307	5.7	18.9
benzene/R1233zdE	4.5	28.9	6.4	0	34	0.38	3.62	3933	220	15.9	20.3
DMC/R1336mzz(Z)	2.4	21.1	8.9	0	41	0.53	3.61	2423	215	13.4	15.8
water/ammonia	1.1	14.3	12.5	0	7	0.84	3.39	1761	539	36.2	21.6
ethanol/m-xylene	0.5	9.9	18.8	7	22	0.43	3.30	718	231	47.4	31.5
cyclobutene	11.0	53.0	4.8	18	30	---	3.38	7704	209	0.0	0.0
R1336mzz(Z)	5.1	35.4	7.0	19	26	---	3.36	3998	218	0.0	0.0
R1233zdE	7.7	42.7	5.6	19	21	---	3.36	5559	349	0.0	0.0
methanol	2.3	29.0	12.8	0	38	---	3.33	3076	234	0.0	0.0
toluene	0.5	6.9	14.3	18	37	---	3.31	590	305	0.0	0.0

ethanol	1.4	22.6	16.3	18	30	---	3.27	1889	231	0.0	0.0

The TH diagrams of toluene/ethanol as refrigerant in the HTHP cycle with and without IHX are compared in Figure 11. The temperature matching in the evaporator for the cycles with and without IHX is similar. For the cycle with an IHX, the refrigerant is further superheated after the evaporator, which resulted in a better temperature match in the condenser. Therefore, a higher COP was obtained for the cycle with an IHX. However, the superheating due to the presence of the IHX also increased the compressor outlet temperature, which is a drawback.

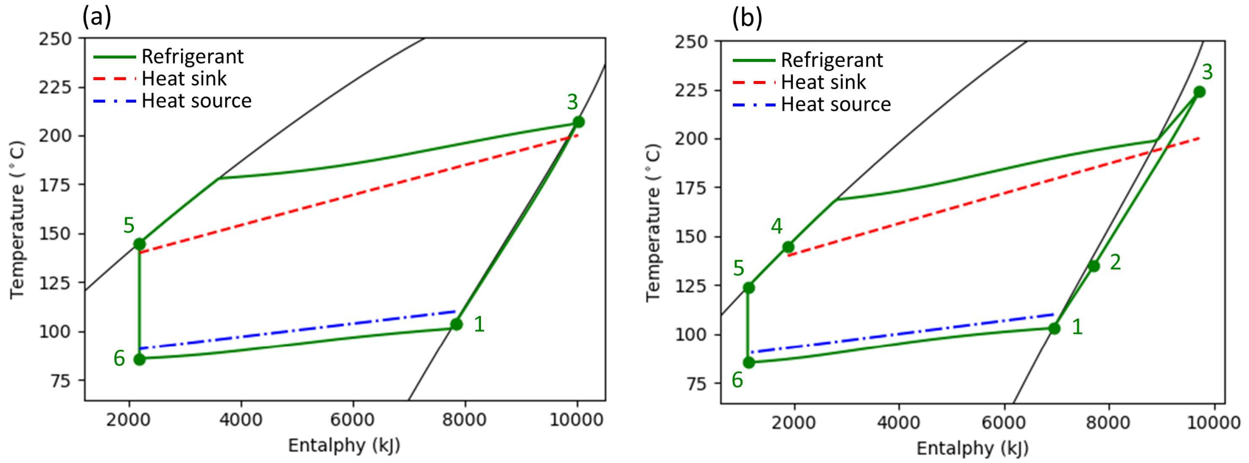

Figure 11. TH diagrams of toluene/ethanol in the HTHP cycle (a) without IHX and (b) with IHX.

While in general the addition of the IHX into the HTHP cycle resulted in an increase in the COP, for some of the mixtures an opposite trend was observed. For example, for the cycle without IHX, water/ammonia was among the top ten mixtures presenting a COP of 3.48. For the cycle with an IHX, the COP for this mixture was reduced to 3.39. The reason is related to the extreme compressor outlet temperature for this mixture, which was increased to even higher values by adding the IHX. The high compressor outlet temperature causes a poor temperature matching at the entrance of the condenser, thus a reduced COP.

It is observed that adding an IHX to the heat pump cycle slightly reduces the compression ratio. For example for toluene/ethanol, the compression ratio was reduced from 11.5 to 9.5. For other mixtures such as water/acetone and methanol/ethyl benzene, the difference between compression ratio of the cycle with and without IHX was lower. Furthermore, by adding an IHX, the superheating of the evaporator is significantly reduced and it is near to zero for most of the mixtures. On the other side, the amount of subcooling did not change significantly compared to the case without IHX. Another interesting result is that in presence of an IHX, the mixtures containing HFOs, such as benzene/R1233zdE and DMC/R1336mzz(Z), appear among the top performing mixtures.

3.4. Challenges with zeotropic mixtures

The performed analysis shows the importance of the process integration to assess the performance of a high temperature heat pump and of the refrigerant used. Based on the results, binary zeotropic mixtures could be theoretically applied in all cases, showing positive aspects compared to pure fluids (e.g. by decreasing the compression ratio or the compressor outlet temperature). However, the main driving parameter remains the temperature glide at the sink and source and only for the third case analyzed (sensible heat exchange both at the source and at the sink) the zeotropic mixtures outperform the pure fluids. Among the others, mixtures with hydrocarbons are the best choice when a high temperature up to 200°C needs to be achieved. However, an interesting result is represented by the behavior of the mixture water/ammonia. It allows to achieve good COP with a positive contribution of the ammonia to reduce the maximum temperature of the cycle and the compression ratio, that are the two main issues to use the natural refrigerant water. Eventually, two aspects need to be considered when analyzing the performance obtainable with binary mixtures. These are: (i) the assessment of thermodynamic properties of mixtures and (ii) the risk of fractionation. These aspects are discussed in detail in the following sections.

3.4.1. Availability of mixing parameters

The estimated physical properties of mixtures are highly dependent on the mixing parameters that are used in the thermodynamic model. In REFPROP, these mixing parameters are available for commonly used mixtures. For the rest of the mixtures, the mixing parameters of a similar mixture is used, or the mixing parameters are estimated based on the Lemmon and McLinden method [39]. For the top performing mixtures, such as toluene/ethanol, ethanol/p-Xylene, water/ethanol and water/ammonia, the mixing parameters are available in REFPROP. However, the mixing parameters are estimated for several other mixtures. This is especially true for mixtures containing HFOs. For the sake of clarity, this can affect the accuracy of such results. However, in order to verify the goodness of this estimation method, a couple of unknown mixtures were tested also experimentally by the authors and the tests demonstrated low differences between the results with real and estimated interaction parameters, reassuring on the validity of the analysis.

3.4.2. Fractionation

As discussed earlier, ΔT_b (the difference in the normal boiling point of the constituent components) is normally used as a measure of fractionation of a binary mixture in refrigeration cycles. For some of the best performing mixtures ΔT_b is quite high, which could be an indication of high risk of fractionation. To investigate this in more detail, the risk of fractionation is compared for four mixtures with different ΔT_b: water/ammonia ($\Delta T_b = 133°\text{C}$), methanol/M-xylene ($\Delta T_b = 75°\text{C}$), toluene/ethanol ($\Delta T_b = 32°\text{C}$) and methanol/cyclopentane ($\Delta T_b = 10°\text{C}$). The variation of relative volatility α for these mixtures along the condenser and evaporator of the HTHP without an IHX is depicted in Figure 12. For all the mixtures except water/ammonia, the variation of α in the evaporator was higher than in the condenser. This could be related to the higher pressure in the condenser, which influences the relative volatility. For methanol/M-xylene, α was increased with a factor six during evaporation, therefore there is a big risk of fractionation. For toluene/ethanol, α was almost doubled during evaporation, showing a lower risk of fractionation compared to methanol/M-xylene. For methanol/cyclopentane, α slightly varied during evaporation, so the chance of fractionation is quite low. Interestingly, water/ammonia did not follow a similar trend. While ΔT_b of water/ammonia is the highest (133°C) among the studied mixtures, α only varied between 14 and 21.5 during evaporation, which is comparable to toluene/ethanol with much lower ΔT_b (32°C). The reason for this contradiction is that apart from ΔT_b, fractionation depends on other parameters such as pressure, mixture composition, and vapor quality at the beginning of evaporation. These results indicate that the fractionation should be studied in detail for each mixture, and a high ΔT_b does not always indicate a high risk of fractionation.

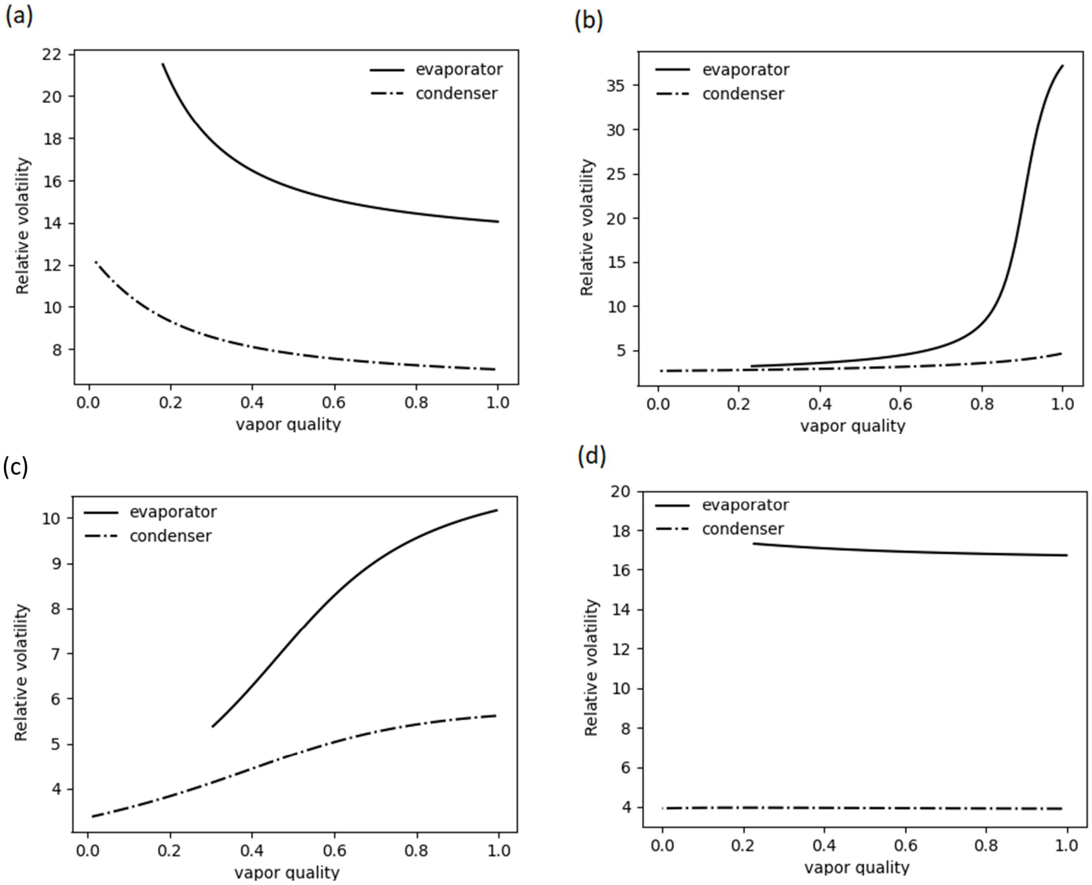

Figure 12. relative volatility versus vapor quality in the evaporator and the condenser for (a) water/ammonia ($\Delta T_b = 133°C$), (b) methanol/M-xylene ($\Delta T_b = 75°C$), (c) toluene/ethanol ($\Delta T_b = 32°C$) and (d) methanol/cyclopentane ($\Delta T_b = 10°C$) mixtures.

4. Conclusions

In this work, the application of binary mixtures as working fluid in HTHPs was investigated. REFPROP10 was used for calculating the physical properties of the binary mixtures. Some screening steps are performed to reduce the number of binary mixtures analyzed. In the first step, mixtures with unfavorable GWP and ODP were removed from the list. Further screening was also done based on critical temperatures of fluids. In this way, the number of binary mixtures was reduced to a computationally approachable value of 1346. An optimization framework able to simulate and optimize heat pump cycles for the selected binary mixtures was developed, considering cycle architectures with and without an internal heat exchanger. The tool optimizes the operating conditions of the heat pump (i.e. p_{ev}, p_{cd}, ΔT_{sh} and ΔT_{sc}) as well as z_{mole} for each binary mixture, in order to maximize the COP. The optimization framework is applied to three relevant industrial cases that are strongly different in terms of source and sink temperature profiles. The distillation case has a negligible temperature glide at both the heat source and sink. The superheated steam drying case has almost no temperature glide at the heat source, but a strong temperature glide at the heat sink. Finally, the pressurized hot water production case has a strong temperature glide at both source and sink.

The main conclusions of the performed analysis are summarized in the following.

- The optimizer identifies the working fluids leading to the highest COP. However, to choose the best working fluid for each of the case studies other parameters such as compression ratio, pressures in the condenser and evaporator, flammability and volumetric heating capacity need to be considered.
- For the distillation case (constant temperature in the heat sink and the heat source), the best performing binary mixtures are near-azeotropic with slightly higher COPs compared to the pure fluids. Binary mixtures also provided some advantages in terms of compression ratio and compressor outlet temperature compared to pure fluids, however it is not normally enough to favor their application.
- In the SSD case, there is a temperature difference in both the heat sink and the heat source. However, given that the input of the source is superheated steam very close to saturated conditions, the source behaves like a latent heat source with small temperature glide. For this case, the best performing binary mixtures were near-azeotropic with slightly higher COPs compared to their constituent compounds. Therefore, for the SSD case, binary mixtures does not provide significant advantages in terms of performance compared to pure refrigerants.
- For the PHWP case (varying temperature in both heat sink and heat source) binary mixtures resulted in higher COPs compared to pure fluids. As an example, the highest COP for the PHWP case without IHX was 3.60 (ethanol/P-xylene), while the highest COP obtained by the pure fluids for the same case was 3.25 (methanol). The average COP for the mixtures was also higher compared to the pure fluids. Moreover, in several cases, VHC for the mixtures was higher than VHC of their constituent compounds. The best performing mixtures are mostly composed of hydrocarbons with high flammability. Water/ammonia was the only natural and mildly-flammable mixture which was present among the top performing mixtures with a COP of 3.48.
- Considering water/ammonia in PHWP case, an analysis based on relative volatility calculations showed that the risk of fractionation for this mixture is not very high, although there is a big difference between the normal boiling point of water and ammonia. There are some challenges in using water/ammonia as the refrigerant in HTHP cycles, e.g. high compressor outlet temperature and high compression ratio, and toxicity of ammonia. However, there are technical solutions available for these challenges at a certain cost.
- Mixtures of an HFO with a hydrocarbon (e.g. R1234ze(Z)/benzene and R1234ze(Z)/acetone) in PHWP case can be also interesting candidates, providing matching temperature glides. However, they are not among the best performing mixtures and they are still flammable. The other studied non-flammable mixtures (mixture of HFOs and CO_2) did not improve the COP compared to their constituent compounds.
- Adding an IHX to the heat pump cycle, on average, resulted in higher COPs, while it did not significantly influence the compression ratio, and in some cases increased the compressor outlet temperature. It was also shown that by adding an IHX to the heat pump cycle, the best performing mixtures were changed significantly. While most of the best performing ones are still hydrocarbons, it was observed that mixtures containing HFOs appear more often at the top of the list. Apart from these positive points, adding an IHX increases the system costs. Therefore, a

financial analysis should be done to decide if the presence of an IHX is advantageous. For water/ammonia adding an IHX to the heat pump cycle produced a lower COP compared to the cycle without an IHX. Moreover, it increases the compressor outlet temperature, which was already high for the cycle without an IHX. Therefore, compared to most of the other investigated mixtures, water/ammonia cycles tend to be more efficient without an IHX, avoiding the extra cost and reducing the complexity of the cycle. In this regard, as future study, it would be interesting to analyze a heat pump architecture with multiple compression steps and intercooling stages in between for water/ammonia and to compare the results with the heat pump with a single compressor.

To conclude, this analysis highlighted the role and potential of binary zeotropic mixtures in high temperature heat pumps. The purpose was not to propose only one suitable refrigerant: it is clear, indeed, from the results that several aspects affect the choice of the refrigerant, especially the boundary conditions. The aim of this work was to show the performance of different fluids when considering some specific representative industrial processes and to clarify the relevance of process integration for an informed refrigerant selection. Further studies will be necessary to combine the technological developments needed (e.g. compressor design, lubricant selection, etc.) with the identification of a refrigerant suitable for high temperature heat pumps for waste heat recovery in industry.

5. Acknowledgement

We gratefully acknowledge the financial support of the Flemish Government and Flanders Innovation Entrepreneurship (VLAIO) through the Moonshot project Upheat-INES (HBC.2020.2616).

References

1. European Commission, “A clean planet for all. A European strategic long-term vision for a prosperous, modern, competitive and climate neutral economy,” 2018.

2. G. P. Thiel and A. K. Stark, “To decarbonize industry, we must decarbonize heat,” Joule, vol. 5, no. 3, pp. 531–550, 2021, doi: 10.1016/j.joule.2020.12.007

3. D. Schüwer and C. Schneider, “Electrification of industrial process heat: Long-term applications, potentials and impacts,” Ecee Ind. Summer Study Proc., vol. 2018-June, pp. 411–422, 2018

4. F. Bühler, F. M. Holm, and B. Elmegaard, “Potentials for the electrification of industrial processes in Denmark,” *ECOS 2019 - Proc. 32nd Int. Conf. Effic. Cost, Optim. Simul. Environ. Impact Energy Syst.*, pp. 2137–2152, 2019.

5. D. Wu, B. Hu, R.Z. Wang. Vapor compression heat pumps with pure Low-GWP refrigerants. Renewable and Sustainable Energy Reviews. 138 (2021) 110571.

6. K.J. Chua, S.K. Chou, W.M. Yang. Advances in heat pump systems: A review. Applied Energy. 87 (2010) 3611-24.

7. M Papapetrou, G Kosmadakis, A Cipollina, U La Commare, G Micale, Industrial waste heat: Estimation of the technically available resource in the EU per industrial sector, temperature level and country, Applied Thermal Engineering 138, 207-216

8. C. Arpagaus, F. Bless, M. Uhlmann, J. Schiffmann, and S. S. Bertsch. High temperature heat pumps: Market overview, state of the art, research status, refrigerants, and application potentials. Energy. 152 (2018) 985–1010.

9. R. de Boer, A. Marina, B. Zuhlsdorf, C. Arpagaus, M. Bantle, V. Wilk, B. Elmegaard, J. Corberan, and J. Benson, Strengthening Industrial Heat Pump Innovation: Decarbonizing Industrial Heat (2020).

10. W.R. Nyemba, S. Chinguwa, B.L. Marango, C. Mbohwa. Evaluation and feasibility assessment of the sustainability of refrigeration systems devoid of harmful refrigerants for storage of vaccines. Procedia Manufacturing. 35 (2019) 291-7.

11. A. Fernández-Moreno, A. Mota-Babiloni, P. Giménez-Prades, J. Navarro-Esbrí. Optimal refrigerant mixture in single-stage high-temperature heat pumps based on a multiparameter evaluation. Sustainable Energy Technologies and Assessments. 52 (2022) 101989.

12. Z. Yang, H. Liu, X. Wu. Theoretical and experimental study of the inhibition and inert effect of HFC125, HFC227ea and HFC13I1 on the flammability of HFC32. Process Safety and Environmental Protection. 90 (2012) 311-6.

13. O. Bamigbetan, T.M. Eikevik, P. Nekså, M. Bantle. Review of vapour compression heat pumps for high temperature heating using natural working fluids. International Journal of Refrigeration. 80 (2017) 197-211.

14 . B. Zühlsdorf, F. Bühler, R. Mancini, S. Cignitti, B. Elmegaard. High Temperature Heat Pump Integration using Zeotropic Working Fluids for Spray Drying Facilities. 12th IEA Heat Pump Conference (2017).

15. O. Bamigbetan, T. Eikevik, P. Nekså, M. Bantle, evaluation of natural working fluids for the development of high temperature heat pumps, The 12th Gustav Lorentzen Natural Working Fluids Conference (2016), PAPER ID 1092.

16. S. Zhang, H. Wang, T. Guo. Evaluation of non-azeotropic mixtures containing HFOs as potential refrigerants in refrigeration and high-temperature heat pump systems. Science China Technological Sciences. 53 (2010) 1855-61.

17. H. Guo, M. Gong, X. Qin. Performance analysis of a modified subcritical zeotropic mixture recuperative high-temperature heat pump. Applied Energy. 237 (2019) 338-52.

18. C. Xu, H. Yang, X. Yu, H. Ma, M. Chen, M. Yang. Performance analysis for binary mixtures based on R245fa using in high temperature heat pumps. Energy Conversion and Management: X. 12 (2021) 100123.

19. D. Roskosch, V. Venzik, J. Schilling, A. Bardow, B. Atakan, Beyond Temperature Glide: The Compressor is Key to Realizing Benefits of Zeotropic Mixtures in Heat Pumps, Energy Technology, 04/2021

20. D. Wang, Y. Wang, B. Yu, J. Shi, J. Chen. Numerical study on heat transfer performance of micro-channel gas coolers for automobile CO2 heat pump systems. International Journal of Refrigeration. 106 (2019) 639-49.

21. E. W. Lemmon, I.H. bell, M. L. Huber, M. O. McLinden, Nist standard reference database 23: reference fluid thermodynamic and transport properties-refprop, version 10.0, national institute of standards and technology, standard reference data program, Gaithersburg (2018).

22. P. Virtanen, R. Gommers, T.E. Oliphant, M. Haberland, T. Reddy, D. Cournapeau, et al. SciPy 1.0: fundamental algorithms for scientific computing in Python. Nature Methods. 17 (2020) 261-72.

23. G. Kosmadakis. Estimating the potential of industrial (high-temperature) heat pumps for exploiting waste heat in EU industries. Applied Thermal Engineering. 156 (2019) 287-98.

24. J.M. Chew, C.C.S. Reddy, G.P. Rangaiah. Improving energy efficiency of dividing-wall columns using heat pumps, Organic Rankine Cycle and Kalina Cycle. Chemical Engineering and Processing: Process Intensification. 76 (2014) 45-59.

25. A.A. Kiss, R.R. Rewagad. Energy efficient control of a BTX dividing-wall column. Computers & Chemical Engineering. 35 (2011) 2896-904.

26. N. Asprion, G. Kaibel. Dividing wall columns: Fundamentals and recent advances. Chemical Engineering and Processing: Process Intensification. 49 (2010) 139-46.

27. R. Sehrawat, P. K. Nema, B. PalKaur. Effect of superheated steam drying on properties of foodstuffs and kinetic modeling. Innovative Food Science & Emerging Technologies. 34 (2016) 285-301.

28. C. Bang-Møller, M. Rokni, B. Elmegaard, J. Ahrenfeldt, and U. Henriksen, Decentralized combined heat and power production by two-stage biomass gasification and solid oxide fuel cells. Energy, 58 (2013) 527–537.

19. A. Mujumdar, handbook of industrial drying. CRC press (2006).

130. C. Mateu-Royo, C. Arpagaus, A. Mota-Babiloni, J. Navarro-Esbrí, S. S.Bertsch. Advanced high temperature heat pump configurations using low GWP refrigerants for industrial waste heat recovery: A comprehensive study. Energy Conversion and Management. 229 (2021) 113752.

31. B. Hu, D. Wu, L.W. Wang, R.Z. Wang. Exergy analysis of R1234ze(Z) as high temperature heat pump working fluid with multi-stage compression. Frontiers in Energy volume 11 (2017) 493–502.

32. EUR-Lex - 32014R0517 - EN - EUR-Lex (europa.eu)

33. American society of heating, refrigerating and air-conditioning engineers, ASHRAE 34: safety standard for refrigeration systems and designation and safety classifications of refrigerants", [online]. Available: HTTPS://WWW.ASHRAE.ORG/TECHNICAL-RESOURCES/BOOKSTORE/STANDARDS-15-34#:~:TEXT=ASHRAE%20STANDARD%2034%20ESTABLISHES%20A%20UNIFORM%20SYSTEM%20FOR,FOR%20REFRIGERANTS%20AND%20TO%20DETERMINE%20REFRIGERANT%20CONCENTRATION%20LIMITS, [Accessed: 11-Fed.-2021].

34. National fire protection association, NFPA 704: standard system for the identification of the hazards of materials for emergency response, [online]. Available: https://www.nfpa.org/CODES-AND-STANDARDS/ALL-CODES-AND-STANDARDS/LIST-OF-CODES-AND-STANDARDS/DETAIL?code=704, [Accessed: 11-Fed.-2021].

35. G. Bamorovat Abadi, K.C. Kim. Investigation of organic Rankine cycles with zeotropic mixtures as a working fluid: Advantages and issues. Renewable and Sustainable Energy Reviews. 73 (2017) 1000-13.

36. M. Chys, M. van den Broek, B. Vanslambrouck, M. De Paepe. Potential of zeotropic mixtures as working fluids in organic Rankine cycles. Energy. 44 (2012) 623-32.

37. J. Shen, H. Tang, Z. Zhang, Z. Xing. Experiment study of a water injected twin screw compressor for mechanical vapor recompression system. 22nd International Compressor Engineering Conference at Purdue, July 14-17 (2014).

38. A. Redón, E. Navarro-Peris, M.Pitarch, J.Gonzálvez-Macia, J.M.Corberán. Analysis and optimization of subcritical two-stage vapor injection heat pump systems. Applied Energy 124 (2014) 231-240.

39. E.W. Lemmon, M.O. McLinden, Method for estimating mixture equation of state parameters, Proceedings of the Thermophysical Properties and Transfer, Processes of New Refrigerants Conference, Paderborn, Germany, (2001). International Institute of Refrigeration, Commission B1, 23-30, ISBN 2-913149-19-7.

Appendix: List of screened fluids

Name	REFPROP NAME	T_b [°C]	T_c [°C]	P_c [°C]	NPFA/ ASHRAE
1,3-Butadiene	13BUTADIENE	-4.5	152.0	43.1	2-4-2-W
1-Butyne	1BUTYNE	8.1	158.9	41.4	1-4-2
1-Pentene	1PENTENE	30.0	192.6	36.0	1-4-1
2,2-Dimethylbutane	22DIMETHYLBUTANE	49.7	216.9	31.4	3-3-0
2,3-Dimethylbutane	23DIMETHYLBUTANE	58.0	227.5	31.6	1-3-0
3-Methylpentane	3METHYLPENTANE	63.2	232.9	31.8	2-3-0
Acetone	acetone	56.1	235.0	46.9	1-3-0
Benzene	benzene	80.1	288.9	49.1	1-3-0
Butane	butane	-0.5	152.0	38.0	A3
Methylcyclohexane	C1CC6	100.9	299.1	34.7	2-3-0
cis-Butene	C2BUTENE	3.7	162.6	42.3	1-4-0
Cyclobutene	cyclobutene	2.6	174.9	51.5	1-4-0
Cyclohexane	CYCLOHEX	80.7	280.5	40.8	1-3-0
Cyclopentane	CYCLOPEN	49.3	238.6	45.8	1-3-1
Octamethylcyclotetrasiloxane	D4	175.7	313.4	13.5	2-2-0
Decamethylcyclopentasiloxane	D5	210.9	345.2	10.9	2-2-0
Decane	decane	174.1	344.6	21.0	1-2-0
Diethyl ether	DEE	34.5	193.6	37.2	A3
Dimethyl carbonate	DMC	90.1	283.9	49.1	1-3-1
Ethylbenzene	EBENZENE	136.2	344.0	36.2	2-3-0
Ethanol	ethanol	78.4	241.6	62.7	2-3-0
Ethylene oxide	ETHYLENEOXIDE	10.5	195.8	73.0	3-4-3
Heptane	heptane	98.4	267.1	27.4	1-3-0
Hexane	hexane	68.7	234.7	30.4	0-3-0
Isohexane	IHEXANE	60.2	224.6	30.4	1-3-0
Isooctane	IOCTANE	99.2	270.9	25.7	0-3-0
Isopentane	IPENTANE	27.8	187.2	33.8	A3
Decamethyltetrasiloxane	MD2M	194.4	326.3	11.4	0-2-1
Octamethyltrisiloxane	MDM	152.5	292.2	14.4	3-1-0
Methanol	methanol	64.5	240.2	82.2	1-3-0
Hexamethyldisiloxane	MM	100.5	245.6	19.3	1-4-0
m-Xylene	MXYLENE	139.1	343.7	35.3	2-3-0
Neopentane	NEOPENTN	9.5	160.6	32.0	2-4-0
Nonane	nonane	150.8	321.4	22.8	1-3-0
Novec 649, 1230	NOVEC649	49.1	168.7	18.7	A3
Octane	octane	125.6	295.6	24.8	1-3-0
Pentane	pentane	36.1	196.6	33.7	A1
Propylene oxide	PROPYLENEOXIDE	34.1	215.0	54.4	3-4-2
p-Xylene	PXYLENE	138.3	343.0	35.3	2-3-0

R1233zd(E)	R1233ZDE	18.3	166.5	36.2	A1
R1234ze(Z)	R1234ZEZ	9.7	150.1	35.3	A2L
R1336mzz(Z)	R1336MZZZ	33.5	171.4	29.0	A1
trans-Butene	T2BUTENE	0.9	155.5	40.3	2-4-1
Toluene	toluene	110.6	318.6	41.3	2-3-0
Ethylene glycol	EGLYCOL	197.2	445.9	105.1	2-1-0
Ethanolamine	MEA	170.4	398.3	81.3	3-2-0
o-Xylene	OXYLENE	144.4	357.1	37.4	2-3-0
water	water	100.0	373.9	220.6	0-0-0
Ammonia	ammonia	-33.3	132.4	113.6	B2L
Carbon dioxide	CO2	-78.5	31.0	73.8	A1
R1234yf	R1234yf	-29.5	94.7	33.8	A2L
R1234ze(E)	R1234ZEE	-19.0	109.4	36.3	A2L
R1243zf	R1243zf	-25.4	103.8	35.2	A2
R161	R161	-37.5	102.1	50.5	0-4-0
R41	R41	-78.3	44.1	59.0	1-4-0

Supplementary material

https://github.com/hamed-Abedini/Supplementary-material.git